Pre-publication manuscript accepted by Mechanical Systems and Signal Processing, January 2008.

Delayed, Multi-Step Inverse Structural Filter for Robust Force Identification

Matthew S. Allen[1] and Thomas G. Carne[2].

[1]*Corresponding Author*
University of Wisconsin-Madison
1500 Engineering Drive, ERB 535
Madison, Wisconsin 53706-1609, USA
msallen@engr.wisc.edu

[2]*Sandia National Laboratories*[*]
P.O. Box 5800, MS 0557
Albuquerque, New Mexico, 87185, USA
tgcarne@sandia.gov

An extension of the Inverse Structural Filter (ISF) force reconstruction algorithm is presented that utilizes data from multiple time steps simultaneously to improve the accuracy and robustness of the ISF. The ISF algorithm uses a discrete-time system model and the measured response to estimate the input forces acting on a structure. The proposed algorithm, dubbed the Delayed, Multi-step ISF (DMISF), is compared with the original ISF and with the Sum of Weighted Accelerations Technique (SWAT) and the classical Frequency Domain Inverse (FD) method in terms of both accuracy and sensitivity to errors in the forward system model. The SWAT and ISF algorithms are capable of estimating the forces acting on a structure in real time, or when time data is available over such a short duration that frequency domain methods cannot be applied effectively. The new DMISF can be created from a forward system model identified by any standard modal analysis algorithm, so one can leverage expertise with a particular system identification methodology. In contrast, the previously presented ISF was derived directly from experimental data. The theory behind the algorithms is presented, after which their performance is demonstrated using laboratory test data. The results of a Monte Carlo simulation are also presented, illustrating the nature of the sensitivity of the methods to errors in the modal parameters of the forward system. The DMISF algorithm is shown to yield a stable inverse system for the structure of interest whereas the traditional ISF is unstable, and hence gives erroneous estimates of the input forces.

Nomenclature

$\{a\}$	=	vector of accelerations
$[\Phi]$	=	matrix of mode vectors
$[W]$	=	weighting matrix for SWAT
$\{x_k\}$	=	discrete time state vector at the kth time instant
$\{y_k\}$	=	discrete time output vector at the kth time instant
$\{u_k\}$	=	discrete time input vector at the kth time instant
[A],[B],[C],[D]	=	system matrices

[*] Sandia is a multi-program laboratory operated by Sandia Corporation, a Lockheed Martin Company, for the United States Department of Energy's National Nuclear Security Administration under Contract DE-AC04-94AL85000.

ω_r	=	modal natural frequency of the rth mode
ζ_r	=	modal damping ratio of the rth mode
λ_r	=	complex modal eigenvalue of the rth mode
$[\Lambda]$	=	diagonal matrix of modal eigenvalues
$\{\psi\}$	=	state space mode vector
$[\Psi]$	=	matrix of state space mode vectors
ω	=	frequency (rad/s)
$[H(\omega)]$	=	Frequency Response Function (FRF) matrix at frequency ω
$[A]_r$	=	modal residue matrix for the rth mode
p	=	number of delays used in DMSIF

1. Introduction

There are countless applications in which it is difficult or impossible to directly measure the dynamic forces acting on a structure, yet knowledge of these forces is vital for analysis and design optimization. In some of these applications it is possible to measure the response of the structure to the unknown forces. Numerous previous works have studied the feasibility of using a structure's response to identify the forces acting on it, in effect, using the structure as its own force transducer [1]. This inverse problem is usually described as ill posed [1, 3]. Its solution can also be very sensitive to small inaccuracies in the data [4-6]; errors in the forward structural dynamic model that seem insignificant in other applications can result in large errors in the computed forces. However, one should be careful and not admit defeat too easily; the forward and inverse problems are different and one should expect that different structural dynamic characteristics will be important in each.

The most commonly used force reconstruction method is a frequency domain technique in which the discrete Fourier transform of the measured responses is multiplied by the inverse (or pseudo-inverse) of the FRF matrix, yielding an estimate of the forces acting on the system. Frequency domain force reconstruction has been studied by a number of researchers [1, 4, 5, 7, 8] The recent work by Hundhausen *et al* [3] provides a comprehensive review.

It is necessary in some applications to have an algorithm capable of estimating the forces acting on a structure in real time. For example, these forces may be required for system control purposes, or the available data may be of such short duration that leakage renders frequency domain processing inaccurate. Also, the challenges in the inverse problem are manifested differently in the time domain, so

it is possible that more accurate or robust solutions could be found by formulating the problem in the time domain. However, it appears that time domain force identification has not been studied as widely as has the frequency domain dual.

A few time domain force reconstruction algorithms have been presented in the literature. One approach is based on modal filtering [9], using multiple sensors on a structure to isolate the portion of a response due to a single mode. This approach, dubbed the Sum of Weighted Accelerations Technique (SWAT), estimates the applied forces by isolating the rigid body modal accelerations [10-12]. It has been extended to estimate multiple forces simultaneously using elastic modes also by Genaro and Rade [2]. Another approach for time domain force reconstruction is based on inverting the equations of motion of the system. For example, the Inverse Structural Filter (ISF) method of Kammer and Steltzner [6, 13-15] inverts the discrete-time equations of motion. The method of Law and Chan is also similar to the ISF although they do not refer explicitly to discrete-time system theory [16]. Others have sought to invert the continuous time equations of motion [17-20] [21]. The discrete time approach is preferred in many cases because it avoids the difficulty associated with integrating or differentiating the measured responses, although one should ensure that proper consideration is given to signal processing [22]. Whichever approach is employed, one can encounter difficulty because the inverse system may have unstable poles, and hence may result in unbounded estimates of the forces.

The ISF presented by Kammer and Steltzner was found from the measured structural impulse response directly, using an approach similar to the Eigensystem Realization Algorithm (ERA) [23, 24], so there was no need to identify a model for the forward system dynamics. On the other hand, as improved methods for identifying forward dynamic models evolved, these could not be easily used with the ISF. In recent years a number of powerful system identification techniques have been developed, so there are now many ways in which a state space model for the forward dynamics of a system can be accurately derived. This work expands upon that by Kammer and Steltzner by deriving a discrete time ISF from a state space model for the forward system, so one can use whatever modal parameter identification method one might prefer.

For the application of interest, the ISF derived from the forward system model was found to be unstable yielding highly erroneous estimates for the forces acting on the structure. A variant is derived, dubbed the Delayed, Multi-step ISF (DMISF) that can produce a stable ISF when the standard method fails. This method also reduces the residual ringing in the ISF estimated forces dramatically. These issues are demonstrated by applying the proposed DMISF to experimental data from a free-free beam and the sensitivity of the method is compared with that of the Frequency Domain inverse method (FD) and the SWAT method.

The primary contributions of this work are the following. First, it presents an extension to a prominent force reconstruction technique that makes it easier to apply and improves its performance. Second, this work provides a comparison between the SWAT and ISF time domain techniques and the frequency domain inverse method. This is especially valuable for the ISF algorithm, which has not previously been compared with any other techniques. Finally, the robustness of all of the methods to errors in the modal parameters of the forward system is demonstrated using a Monte-Carlo simulation.

The next section presents the theory behind the ISF and describes the enhancements mentioned previously. The SWAT and FD algorithms are also briefly discussed. In Section 3, all of the methods are applied to data from an aluminum beam and their characteristics and sensitivity to errors discussed. Some conclusions are presented in Section 4.

2. Force Identification Methods

The following section presents the ISF method of Kammer and Steltzner and discusses the difficulties that can be encountered. Section 2.2 presents an extension to the ISF that has been found to improve its performance. Sections 2.3 and 2.4 briefly present the SWAT and FD methods, which will be compared to the proposed ISF in Section 3.

2.1. Inverse Structural Filter (ISF) of Kammer & Steltzner

An ISF can be derived by inverting the discrete time equations of motion, resulting in a dynamic system that takes a structure's response as input and returns an estimate of the forces acting on the

structure as output [6, 13-15]. The filter is itself a dynamic system, so one can use traditional system analysis methods to evaluate its dynamic performance. For example, one can examine the eigenvalues of the ISF's characteristic equation to evaluate the stability of the ISF.

To derive the basic ISF algorithm, we begin with the familiar linear, state-space, discrete time representation for a dynamic system:

$$\begin{aligned} \{x_{k+1}\} &= [A]\{x_k\} + [B]\{u_k\} \\ \{y_k\} &= [C]\{x_k\} + [D]\{u_k\} \end{aligned} \tag{1}$$

where the state vector $\{x\}$ is N *x 1*, the input vector $\{u\}$ is N_i *x 1*, and the output vector $\{y\}$ is N_o *x 1*. The index k refers to the kth time step for which $t_k = kT_s$ where T_s is the time between successive time samples. For structural dynamic systems, the forces acting on a structure at a set of points are typically the inputs, and the displacement, velocity, or acceleration measured at a set of points are considered the outputs. Peeters [25] gives a good review of various forms of the state-space equations for continuous and discrete time dynamic systems, as well as their relationships to the familiar modal and second order (i.e. mass, stiffness and damping) representations. The discrete time system reproduces the response of its continuous time dual at the sample instants exactly only if the input obeys the assumption used in deriving the discrete time model [26]. For example, the zero order hold (ZOH) assumption is typically used, which assumes that the input is constant between sample instants.

Steltzner and Kammer noted that it is possible to invert the state space representation in eq. (1) as follows

$$\begin{aligned} \{x_{k+1}\} &= [\hat{A}]\{x_k\} + [\hat{B}]\{y_k\} \\ \{u_k\} &= [\hat{C}]\{x_k\} + [\hat{D}]\{y_k\} \\ \hat{A} &= A - BD^+C \quad \hat{B} = BD^+ \\ \hat{C} &= -D^+C \quad \hat{D} = D^+ \end{aligned} \tag{2}$$

where $()^+$ denotes the Moore-Penrose pseudo-inverse. Equation (2) represents a discrete time dynamic system that takes the response $\{y\}$ as input and returns an estimate of the forces $\{u\}$ acting on the system

as output. This can also be expressed as a discrete filter that acts on the sampled response measurements returning a sampled estimate of the forces. Note that the system matrix $\left[\hat{A}\right]$ of the ISF is different than that of the forward system, so the ISF can be unstable even when the forward system is stable.

While Steltzner and Kammer derived the ISF as described above, they did not actually use this procedure to implement the ISF. Instead, they presented an algorithm that computes the Markov parameters of the ISF directly from response data [15]. The Appendix discusses how to generate an inverse structural filter from modal parameters obtained in a standard modal test, using a modal representation of equation (2). This approach was used in this work do derive an enhancement to the ISF.

2.2. Delayed Multi-step ISF (DMISF)

One important difficulty often encountered when implementing the Inverse Structural Filter method is that the ISF system can be unstable. If any of the eigenvalues of the ISF system in eq. (2) are unstable, the estimated forces might tend towards infinity when the ISF is applied to the measured responses. One can see in eq. (2) that the direct transmission matrix [D] contributes to the ISF's eigenvalues. The forward system can be decomposed into a diagonal matrix of eigenvalues [Λ] and a matrix of mode vectors [Ψ]. Equation (16) in the Appendix shows that the [D] matrix depends on the real part of the triple [Ψ][Λ][Ψ]^T, which one can show to depend primarily on the real parts of both the eigenvalues and mode vectors. However, the real parts of both tend to be small and difficult to accurately estimate for a lightly damped structure [23], so the accuracy of the real part of the triple [Ψ][Λ][Ψ]^T in [D] in eq. (16) could also be brought into question. The authors have found that better results are usually obtained if the output is stepped forward one sample and the direct transmission matrix [D] is neglected, resulting in the following delayed state space representation.

$$\begin{aligned}
&\{x_{k+1}\} = [A]\{\dot{x}_k\} + [B]\{\dot{u}_k\} \\
&\{\ddot{y}_{k+1}\} = [C]\{\dot{x}_{k+1}\} + \cancelto{0}{[D]}\{\dot{u}_{k+1}\} = [C_d]\{\dot{x}_k\} + [D_d]\{\dot{u}_k\} \\
&[C_d] = [C][A] \quad [D_d] = [C][B]
\end{aligned} \tag{3}$$

The ISF for this system, generated using eq. (2), estimates the derivative of the input at time t_k from the response at the next time instant t_{k+1}. While this approach tends to improve the performance of the ISF significantly, it is often not sufficient to obtain a stable ISF. For example, eq. (3) produced an unstable ISF for the system considered in the following section.

Steltzner and Kammer [15] found that it was possible to create a non-causal ISF that was more stable and/or more accurate than the standard one. (The non-causal ISF used future values of the response to estimate the forces at the present time.) In that same spirit, if one can tolerate a delay before the forces are estimated, then one can modify the formulation of the ISF to reposition the poles of the ISF system. For example, the authors have found that the following method tends to increase the damping in the ISF's poles, and have dubbed this new method the Delayed Multi-step ISF (DMISF)

Consider forward state equation (3). The following modified output equation results after stacking the input and output for various time instants.

$$\begin{Bmatrix} \{\ddot{y}_{k+1}\} \\ \{\ddot{y}_{k+2}\} \\ \vdots \\ \{\ddot{y}_{k+p}\} \end{Bmatrix} = \begin{bmatrix} [C_d] \\ [C_d][A] \\ \vdots \\ [C_d][A]^{p-1} \end{bmatrix} \{\dot{x}_k\} + \begin{bmatrix} [D_d] & [0] & \cdots & [0] \\ [C_d][B] & [D_d] & \ddots & [0] \\ \vdots & \ddots & \ddots & [0] \\ [C_d][A]^{p-2}[B] & [C_d][A]^{p-3}[B] & \cdots & [D_d] \end{bmatrix} \begin{Bmatrix} \{\dot{u}_k\} \\ \{\dot{u}_{k+1}\} \\ \vdots \\ \{\dot{u}_{k+p-1}\} \end{Bmatrix},$$
$$\{\ddot{y}^S_{k+1}\} = [C_{dm}]\{\dot{x}_k\} + [D_{dm}]\{\dot{u}^S_k\} \tag{4}$$

The state equation must be modified slightly to accommodate the new definition of the output and input

$$\begin{aligned} \{x_{k+1}\} &= [A]\{\dot{x}_k\} + [B][P]\{\dot{u}^S_k\} \\ [P] &= \begin{bmatrix} [I] & [0] & \cdots & [0] \end{bmatrix} \end{aligned} \tag{5}$$

The DMISF generated from this system representation estimates the input at time instants t_k to t_{k+p-1} from the output at time instants t_{k+1} to t_{k+p}. This is applied to the output at t_k to t_{Nt-p} resulting in multiple estimates for each of the input forces. The most important feature of this method is that it provides an avenue by which one can find a stable ISF system when that produced by eq. (2) or (3) is unstable. The

matrix [D] on which the ISF's stability depends has been replaced with [D_{dm}], which one can modify by increasing p until a stable ISF is obtained.

Unfortunately, no simple method has materialized by which one prove that the DMISF produces a more heavily damped and hence a more stable inverse system than the original ISF in every case, although this has been observed empirically. For example, the DMISF as presented here has been found to give excellent results relative to other force identification algorithms, as demonstrated in Section 3. The authors demonstrated in [10] that one could place the poles of the ISF arbitrarily simply by modifying the output equation, so long as the number of outputs was greater than the number of system poles. Unfortunately, this is often not the case. One could also resort to nonlinear optimization to attempt to place the system poles (see the Appendix in [10]). Compared to these other methods, the DMISF gives a simple yet effective avenue to explore when seeking a stable ISF for a particular system, since only the delay p need be modified to improve its stability.

2.3. Sum of Weighted Accelerations (SWAT)

The Sum of Weighted Accelerations Technique (SWAT) was presented by Carne *et al* [12], although the method had been developed previously by Gregory, Priddy and Smallwood [27, 28]. It has been successfully applied to a number of systems [11, 29, 30]. The technique is based upon the concept of a modal filter. The rigid body mode shapes, along with the mode shapes of the elastic modes in the frequency band of interest are used to construct a spatial filter that removes the flexible modes from the response, leaving only the rigid body accelerations. This spatial filter is simply a weighting matrix that isolates the rigid body accelerations in the response. If the mass properties of the structure are known, the rigid body accelerations can be multiplied by the mass properties to obtain an estimate of the sum of the forces and moments acting at the body's center of gravity. In some cases the free, unforced response, which is a linear combination of the elastic mode shapes, can be used to generate an adequate spatial filter (i.e. the SWAT-TEEM algorithm [12, 30]), eliminating the need for modal parameter identification. The primary limitation of the SWAT algorithm is that it requires that the number of sensors be at least as great

as the number of rigid body modes plus the number of elastic modes and that the sensors are well placed so that the filtering problem is well conditioned.

It is also important to note that the SWAT algorithm determines the equivalent forces and moments that, if applied at the center of mass, would cause the same acceleration of the center of mass, and does not identify the spatial distribution of the applied forces directly. One would expect that this feature might make the SWAT algorithm more robust than the alternatives when the locations of the applied forces are unknown, because it is likely to be easier to estimate the sum of the forces rather than the individual forces themselves. If the location at which the force is applied is accurately known and the number of applied forces is less than or equal to the number of rigid body modes, this may be sufficient to determine the individual forces. Genaro and Rade [2] presented an extension of SWAT that also uses the elastic modes to identify the forces, so it can identify the forces at individual response points provided that the number of modes in the frequency band of interest exceeds the number of forces desired.

The SWAT algorithm is derived in [11, 12, 29] and explained in the context of the modal filter. An alternate derivation will be summarized here. We begin by approximating the measured acceleration as a sum of modal contributions as follows

$$\{a\} = [\Phi]\{\eta\} \tag{6}$$

where $\{a\}$ is an N_0 x 1 vector of accelerations at the measurement points, $\{\eta\}$ is an N x 1 vector of modal displacements, $[\Phi]$ is an N_0 x N matrix of mode shapes and N_o and N are the number of measurement points and modes respectively. Let N_{RB} denote the number of rigid body modes. An N_o x N_{RB} weighting matrix [W] is sought that, when multiplied with the measured accelerations, extracts an N_{RB} x 1 vector of rigid body accelerations $\{a_{RB}\}$.

$$\{a_{RB}\} = [W]^T \{a\} \tag{7}$$

If the rigid body mode vectors are mass normalized and assigned to the leading columns of $[\Phi]$, then equation (6) can be rewritten as

$$\{a\} = \left[\begin{bmatrix} \Phi_{RB} \end{bmatrix} \quad \begin{bmatrix} \Phi_e \end{bmatrix} \right] \begin{Bmatrix} \{a_{RB}\} \\ \{\ddot{\eta}_e\} \end{Bmatrix} \tag{8}$$

where the matrices represent the rigid body and elastic modes respectively and $\{\eta_e\}$ is the vector of elastic modal coordinates corresponding to the modes in $[\Phi_e]$. Combining equations (8) and (7) and with the requirement that $[W]^T$ nullify the elastic modes while extracting the rigid body accelerations yields

$$\begin{aligned} [W]^T \left[\begin{bmatrix} \Phi_{RB} \end{bmatrix} \quad \begin{bmatrix} \Phi_e \end{bmatrix} \right] &= \left[\begin{bmatrix} I \end{bmatrix}_{N_{RB} \times N_{RB}} \quad \begin{bmatrix} 0 \end{bmatrix}_{N_e \times N_{RB}} \right] \\ [W] &= \left(\left[\begin{bmatrix} \Phi_{RB} \end{bmatrix} \quad \begin{bmatrix} \Phi_e \end{bmatrix} \right]^T \right)^+ \begin{bmatrix} \begin{bmatrix} I \end{bmatrix}_{N_{RB} \times N_{RB}} \\ \begin{bmatrix} 0 \end{bmatrix}_{N_e \times N_{RB}} \end{bmatrix} \end{aligned} \tag{9}$$

where $()^+$ denotes the pseudo-inverse. One would expect to be able to find a solution that nullifies the elastic modes (or extracts the pure rigid body accelerations) whenever the N_{RB} vectors comprising $[W]$ can be extracted from the null space of the transpose of the elastic mode matrix $[\Phi_e]^T$. This will always be possible whenever $N_o \geq N+N_{RB}$. One should recall that equation (6) is an approximation because any continuous system has, in reality, an infinite number of modes.

The rigid body accelerations are multiplied by the rigid body mass properties yielding the sum of the forces applied to the body. The interested reader may refer to the derivations in [11, 12, 29], which emphasize the importance of sensor selection by describing the algorithm in the context of a modal filter.

2.4. Frequency Domain Inverse Method

By far the most common inverse method used is the frequency domain inverse method. This is based on the following relationship between force and response.

$$\underset{N_o \times 1}{\{Y(\omega)\}} = \underset{N_o \times N_i}{[H(\omega)]} \underset{N_i \times 1}{\{F(\omega)\}} \tag{10}$$

The use of frequency domain data usually implies that the responses have been measured over a sufficiently long time that they can be transferred to the frequency domain via a Discrete Fourier Transform.

Typically, the number of output or response locations exceeds the number of force or input locations, so the inverse problem is over-determined. The forces are obtained by multiplying both sides of the equation by the pseudo-inverse of *[H(ω)]*.

$$\underset{N_i\times 1}{\{F(\omega)\}} = \underset{N_i\times N_o}{\left[H(\omega)\right]^{+}} \underset{N_o\times 1}{\{Y(\omega)\}} \tag{11}$$

The primary difficulty in applying this method stems from the fact that the FRF matrix tends to be dominated by a rank-one component corresponding to a single mode near the natural frequencies of a system. As a result, the inverse of the FRF matrix can be ill conditioned near the natural frequencies of the system, thus amplifying the effect of measurement errors [5]. Also, away from resonance the FRFs may be well conditioned but they may be dominated by noise since the signal away from resonance is often weak.

The FRF matrix in eq. (10) could consist of measured data, or could be reconstructed from a modal model for the system. The latter approach was used in the results that follow so that all methods are constructed from identical data, the modal model for the forward system.

3. Experimental Results

This section applies the force reconstruction algorithms to data acquired from a 183 cm long aluminum beam, which is suspended by soft bungee cords to simulate free-free boundary conditions. The beam cross section was 2.5 cm high by 3.8 cm wide. Seven pairs of accelerometers were mounted along the length of the beam, spaced 30.5 cm apart. Each pair contained one accelerometer mounted in the vertical direction and one in the axial direction. Figure 1 shows a schematic of the measurement setup. The accelerometers are represented by cylinders and the location at which the force was applied is shown with an arrow.

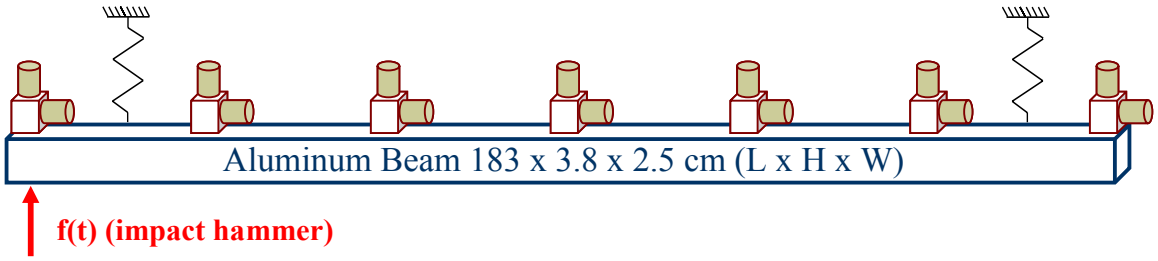

Figure 1: Schematic of system under test.

An instrumented hammer was used to excite the beam and record the force imparted. The measured force and response spectra were used to estimate the frequency response functions of the beam, which were processed using the Algorithm of Mode Isolation (AMI) [31-33]. AMI returned a set of modal parameters describing the dynamics of the beam from 0 Hz to 1500 Hz. System identification was not attempted beyond 1500 Hz because the excitation was relatively weak and so the FRFs were noisy at higher frequencies.

A separate set of data was also taken in which the beam was excited once with an instrumented hammer and the response recorded, sampled at 8192 Hz. The force reconstruction algorithms were then applied to the response data, as described subsequently, and in each case the reconstructed force was compared to the force measured by the hammer.

3.1. Forward System Identification

The Algorithm of Mode Isolation (AMI) [34] was used to find the modal parameters for the beam. A complex modal model was fit to the data in a previous work [10], yet it was later determined that the apparent complexity in the modes was due to small imperfections in the signal processing hardware and that a real mode model was indeed more appropriate. As a result, the real parts of the modal residues returned by AMI were discarded in all of the following, resulting in a classically damped, real mode model for the system. Figure 2a compares the measured drive point FRF with that reconstructed from the real mode model. Figure 2b displays composites of the measured FRFs, AMI's reconstruction, and a composite of the difference between the two. (A composite FRF is defined as the average of the magnitude of all of the FRFs.) A low-frequency residual term was used when curve fitting the FRFs in order to describe the rigid body dynamics of the system and improve the fit near the zeros of the FRFs.

The primary motivation for including this low-frequency residual term when fitting complex modes to the FRFs was to assure that the dynamic model used to generate the ISF system contained a representation of the dynamics of the rigid body modes. This was accomplished by assigning the real part of the low frequency residual term a very low frequency eigenvalue and including it in the state space representation in eq. (16). (If this term was omitted, the forces identified by the ISF contained spurious low-frequency components of very high amplitude.) Note that the zeros of the measured and reconstructed FRFs agree very well at the drive point. The same was observed in the FRFs at other points. The composite of the reconstructed FRFs also agrees quite well with the measured FRFs, although the difference plot in Figure 2b shows large spikes at the natural frequencies, indicating that the agreement is not perfect at the natural frequencies.

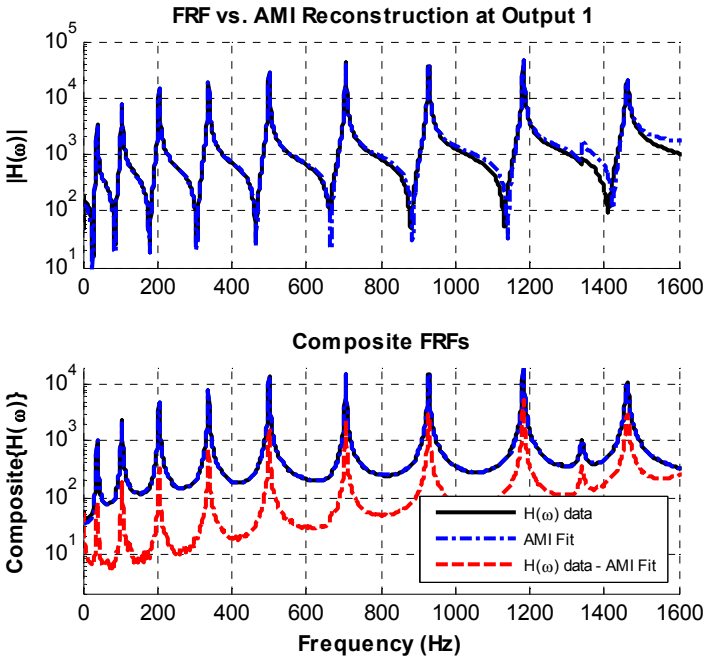

Figure 2: a.) Measured Drive Point FRF $H_{1,1}(\omega)$ vs. AMI Reconstruction – Real Modes. b.) Composites of Measured FRFs, AMI's Reconstruction and of the difference between the two – Real Modes.

3.1.1. Discussion

The discussion of the system identification procedure was presented here in order to highlight some of the details that had to be considered to get a modal model that would be suitable for force reconstruction. Attention was given assure that the zeros of the reconstructed FRFs agreed well with the measurements.

The steps taken here to arrive at a good real mode model improved the identified forces dramatically. The authors are not aware of any analogous operations that can be performed using Kammer and Steltzner's technique, which identifies the ISF directly from the measured data. In fact, the authors have observed that many system identification techniques typically give poor results at the zeros of the FRFs in order to more fully minimize their least squares objective function.

Differences are observed at the resonant peaks in Figure 2 between the data and the reconstructed FRF. These differences were much smaller when a complex modal model was used, as shown in [10], yet this was an artifact due to phase distortions in the measurement system. The model with complex mode vectors did not agree well at the zeros of the FRFs, and when the complex mode model was used in the force reconstruction algorithms it yielded less accurate forces than those that will be presented here. This is an advantage of the DMISF method presented here. The method of Kammer and Steltzner does not allow one to force real modes on the system model, so the spurious complexity in the mode vectors must be retained.

3.2. Inverse Structural Filter

3.2.1. Kammer & Steltzner's Impulse Response based ISF

As discussed previously, Steltzner and Kammer [15] derived a convolution representation for the ISF system directly from the measured impulse response (i.e. from the Markov parameters) rather than using eq. (2). This method was implemented using the inverse FFT of the measured frequency response functions as primary data. Steltzner and Kammer suggested trying various non-causal leads to improve the performance of the ISF system. Experimentation revealed that the best results were obtained using a non-causal lead of 5 samples with 50 terms in the convolution equation. Figure 3 compares the force identified by this ISF to the measured force. During the first 22 milliseconds the ISF force tracks the measured force very well. The ISF estimate becomes highly oscillatory after the force pulse has ceased. Various filter lengths and non-causal leads were investigated, although none resulted in better agreement between the measured and reconstructed forces than that shown in Fig. 3.

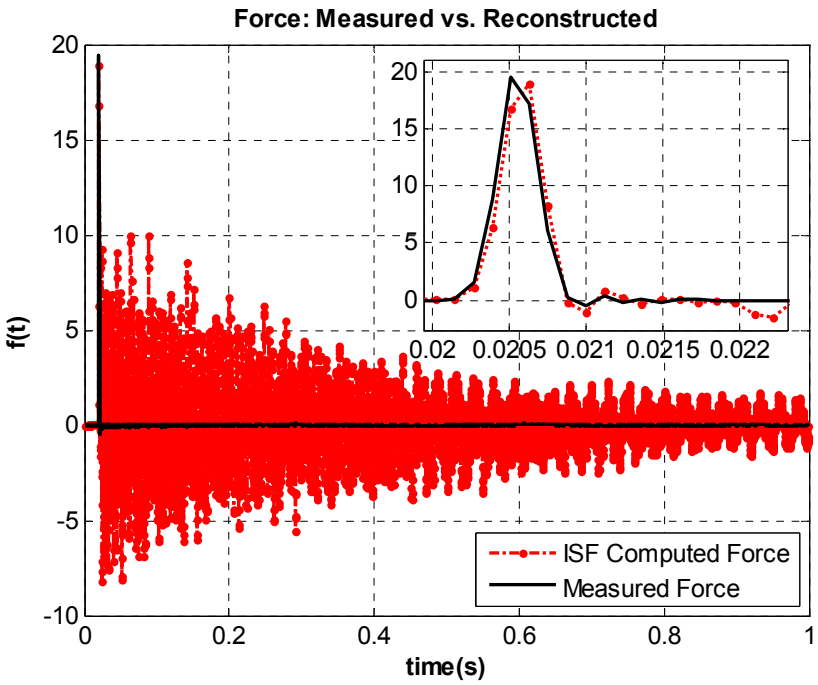

Figure 3: Input force at Node 1 estimated by ISF compared to measured force.

3.2.2. DMISF Derived from Experimental Modal Model

A delayed, multi-step ISF (DMISF) was also constructed from the identified state space model, as described in Section 2.1.3, and then applied to the measured response data for the beam. Six delays (p=6 in eq. (4)) were used. This was the smallest p that was stable for the real mode model presented in Section 3.1. The method presented in eq. (3) worked for the complex modes, as shown in [10], but yielded an unstable ISF when real modes were used. Figure 4 compares the force returned by the DMISF with the measured force. The inverse FFT of the force obtained by the frequency domain inverse method (FD) is also shown. Both methods agree well with the measured force, yet both methods show some residual ringing after the force had ceased. However, the residual ringing in the FD and DMISF forces is considerably less than for the impulse-response derived ISF in Figure 3.

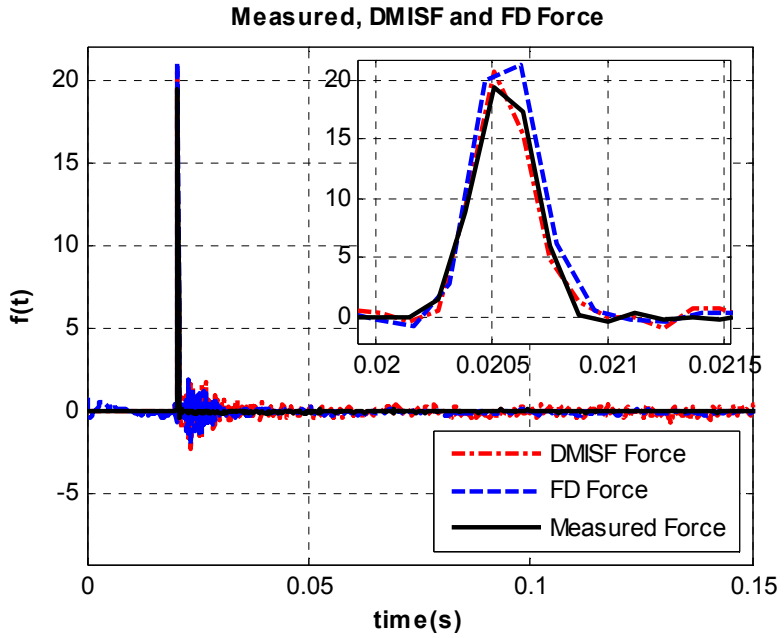

Figure 4: DMISF Force, FD Inverse Method Force, and Measured Force in the time domain. The Nyquist Frequency was 3200 Hz and no filtering was applied to the signals.

3.3. Sum of Weighted Accelerations Technique (SWAT)

The SWAT algorithm was also applied to the data from the beam. The real mode vectors found in Section 3.1 were used in conjunction with analytically derived rigid body mode shapes in eq. (9) to find the SWAT weights. There are a number of analyses that one can perform prior to applying SWAT to a set of response data in order to predict how it will perform. First, the SWAT algorithm can be applied to the measured FRFs, which were used to identify the mode vectors of the system, resulting in what has been called SWAT FRFs [11, 12]. This is done by multiplying the SWAT weights in eq. (9) with the measured FRF matrix. The measured FRFs represent the response due to a flat, unit force (or unit impulse force), so the SWAT FRFs thus obtained should be constant for all frequencies. Visual inspection of the SWAT FRFs typically gives a good indication of the ability of SWAT to isolate the rigid body accelerations of the structure using the given sensor set.

Figure 5 shows the SWAT FRFs for the two dominant rigid body modes present in the data, rigid body translation in the vertical direction and rigid body rotation. The SWAT FRFs are essentially flat up to about 600 Hz, and decrease slowly between 600 and 1200 Hz, deviating wildly above 1500 Hz. The decreasing trend between 600 and 1200 Hz, which is reminiscent of the effect of an out of band mode, was even more severe in [10]. This effect was reduced in this work by fitting a residual flexibility to the measured FRFs and including it as if it were another mode vector when computing the SWAT weights. (The residual flexibility has the form $UR*\omega^2$ where UR is a constant, see [23] or [35].) The SWAT FRFs clearly indicate that one will not obtain accurate results using this sensor set without first low pass filtering the response data to minimize the frequency content to below about 1200 Hz.

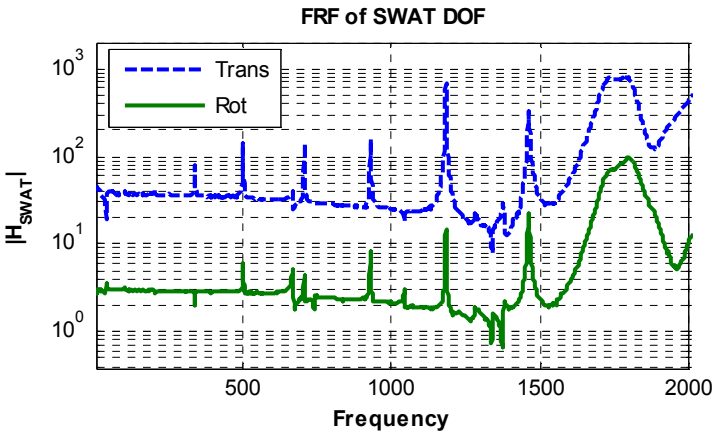

Figure 5: FRF for SWAT degrees of freedom, rigid body translation and rigid body rotation (or pitch.) including an upper residual term when deriving the SWAT weights.

This can be explained by examining the linear independence of the mode vectors that were used to derive the SWAT weights (on the measurement point set). Figure 6 shows a plot of the Modal Assurance Criterion Matrix or MAC Matrix [36] between these modes. (The MAC between two vectors gives an indication of their linear independence. A value of zero indicates perfect independence, or vectors that are orthogonal in a Euclidean sense, while a value of one indicates that the vectors are multiples of each other.) The off-diagonal MAC values (i.e. the MACs between the different mode vectors) are above 0.5 for a number of the mode vector pairs, suggesting that a larger number of measurement points are needed to fully distinguish them from one another.

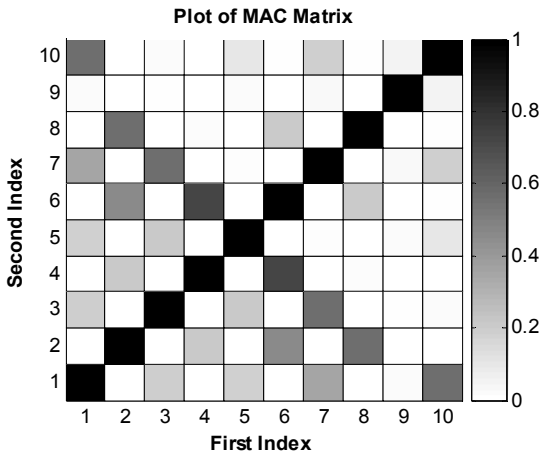

Figure 6: Plot of MAC matrix between modes identified by AMI – Real Modes.

The SWAT FRFs indicate that the modal filter that SWAT uses to determine the forces is only reliable out to about 1000 Hz for this sensor set. However, the measurement set is sufficient to get good results with the ISF and FD algorithms over the entire 0 to 1500 Hz band of interest and quite reasonable results are even obtained using the entire measured band (0 to 3200 Hz). From this point forward the response data used by all methods will be low pass filtered using a high order Butterworth filter with a cutoff frequency of 1000 Hz in order to limit the forces to a subset of the system identification band, since this is the procedure that one should adopt in practice.

3.3.1. Discussion

It is interesting to note that the frequency at which the SWAT FRFs begin to deviate significantly from unity, 600 Hz, happens to be just above the natural frequency of the 5th elastic mode (500 Hz). Most of the motion for this structure was in the vertical direction. With seven accelerometers in this direction and two rigid body modes, one would expect to be able to eliminate only five elastic modes. The off diagonal terms involving the sixth and higher modes suggest that the seven axial accelerometers do not provide sufficient additional information to distinguish the sixth and higher modes from the first five. This seems to confirm the rule of thumb that states that one should have at least one measurement point per mode in the frequency band of interest to get accurate results with SWAT. The previous discussions have also highlighted the great utility of the SWAT FRFs both in providing an *a priori* indication of the expected accuracy of the identified forces and as a diagnostic tool.

3.4. Comparison of All Methods and Discussion of Results

Figure 7 compares the force time histories identified by all of the methods. All have been filtered with a cutoff frequency of 1000 Hz to limit the data to a fraction of the frequency band in which system identification was performed. The algorithms all show about the same level of residual ringing after the true force has ceased. The inset shows an expanded view of the force at early times. The SWAT algorithm underestimates the force by about 15% while the FD method overestimates it by about 20%. The DMISF computed force overlays the measured force. The impulse response based ISF [6, 14, 15]was shown in Figure 3, yet is not repeated here because it showed excessive ringing after the force pulse had ceased. As noted in Section 2.1 and 2.2, an ISF could have also been created using eq. (2), yet this resulted in an ISF with 17 poles outside of the unit circle, and hence gave unbounded forces, even when the non-causal approach in eq. (3) was used, so this approach will not be presented here.

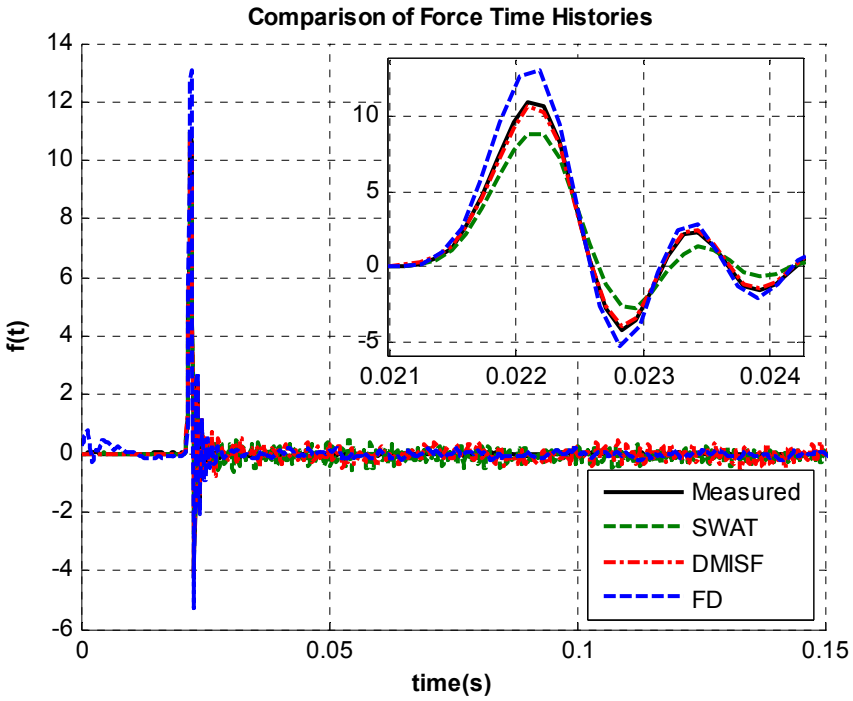

Figure 7: Comparison of time domain forces identified by all methods, all filtered with a cutoff frequency of 1000 Hz.

Figure 8 compares the force spectra identified by each of the methods discussed in this paper. Markers are also displayed indicating the natural frequencies of the forward system (crosses) and the ISF system (circles). Both the ISF and FD forces show spikes at many of the natural frequencies of the

forward system. The ISF force also shows large, narrow band deviations from the measured force at many of its poles. The largest of these deviations occur at 460 and 660 Hz. These frequencies correspond to those of the two poles of the ISF system that were unstable for smaller delays ($p < 6$) and for the method in Section 2.1. The spectrum identified by SWAT is the smoothest and is quite accurate below 500 Hz yet it deviates from the measured spectrum a fair amount above 500 Hz, underestimating the force by 75% at 900 Hz. It was noted previously that the number of accelerometers used is suspected to be insufficient to obtain optimal results with SWAT above about 600 Hz. A higher cutoff frequency was used in Figures 8 and 7 in order to facilitate comparison with the other methods and to demonstrate the magnitude of the error incurred by extending the frequency range of the SWAT algorithm slightly beyond the flat region of the SWAT FRFs. The DMISF and FD methods track the force spectrum more closely above 500 Hz, yet they also show a number of spurious peaks.

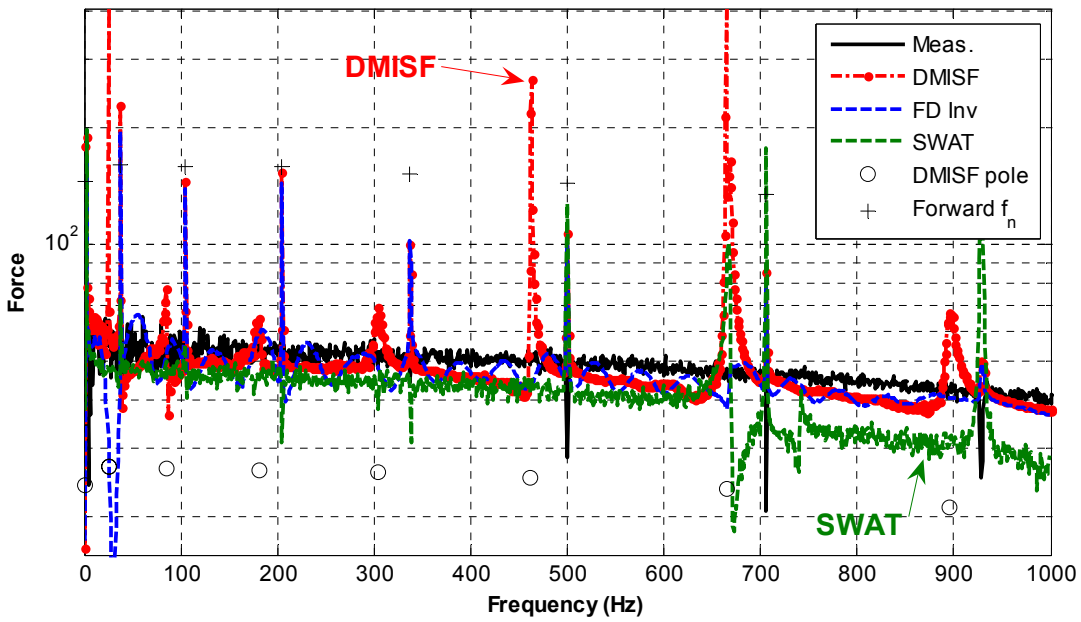

Figure 8: Comparison of force spectra identified by all methods.

3.5. Sensitivity to Errors in Identified Model

The sensitivity of all of the methods was studied using Monte Carlo simulation. The modal natural frequencies, damping ratios and residues identified were each perturbed by independent, uniform random numbers to span ±0.5%, ±5% and ±5% respectively of their identified values. These values are meant to

be typical of error bounds encountered in modal parameter identification [36, 37]. The forces acting on the beam were then computed using the DMISF, SWAT and FD methods using the perturbed modal parameters. This was repeated for thirty different sets of random perturbations. The range spanned by the identified forces as a function of time and frequency was then stored.

Figure 9 shows the range of forces identified as a function of time for each of the methods. Each color band represents the maximum and minimum force observed at each particular time for the ensemble of thirty responses. Nine delays were used in the Monte Carlo simulation (p=9) because it was found that the DMISF with p=6 was sometimes unstable for some of the trials (i.e. for some combinations of the perturbed modal parameters). The responses used as input data in this study were filtered with a cutoff frequency of 1000 Hz in order to limit the contribution of the response above the frequency band that was used in system identification. Once again, each algorithm showed about the same level of residual ringing, so only the early time results are presented. The Monte Carlo simulation shows that the time response estimated by the DMISF algorithm is no more sensitive to errors in the forward system model than that estimated by the FD or SWAT algorithms; all methods show about the same level of scatter as a function of time.

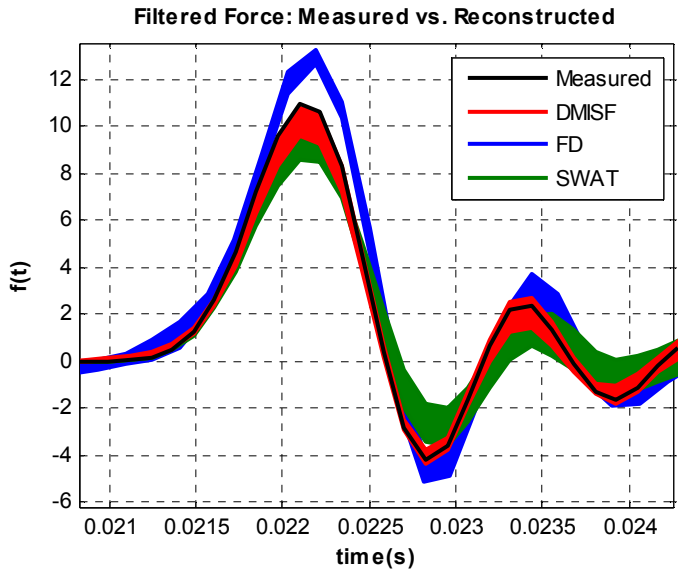

Figure 9: Range of forces found versus time for DMISF, Frequency Domain Inverse method and SWAT with errors in the forward system parameters.

Interestingly, the FD and SWAT estimates do not encompass the measured force for the assumed uncertainty model. This suggests either that the error model for the forward system is innacurate, or that the methods yield a significant bias in the presence of random errors. On the other hand, the range of the DMISF forces includes the measured force over this time window, although the measured force is near the edge of the range during the force pulse.

Figure 10 shows the range of the force amplitude spectra of the forces in Fig. 9. Lines are shown representing the maximum and minimum forces identified by the DMISF, SWAT and FD methods. The measured force is shown in each pane to aid in the comparison. The SWAT algorithm shows somewhat more variability at high frequencies and the mean of the SWAT forces underestimates the true force spectrum significantly at higher frequencies. The Frequency domain inverse method and the DMISF show similar levels of uncertainty, with the largest uncertainties at the structure's natural frequencies. The DMISF algorithm also exhibits relatively large uncertainty at its poles (denoted by circles in Fig. 10).

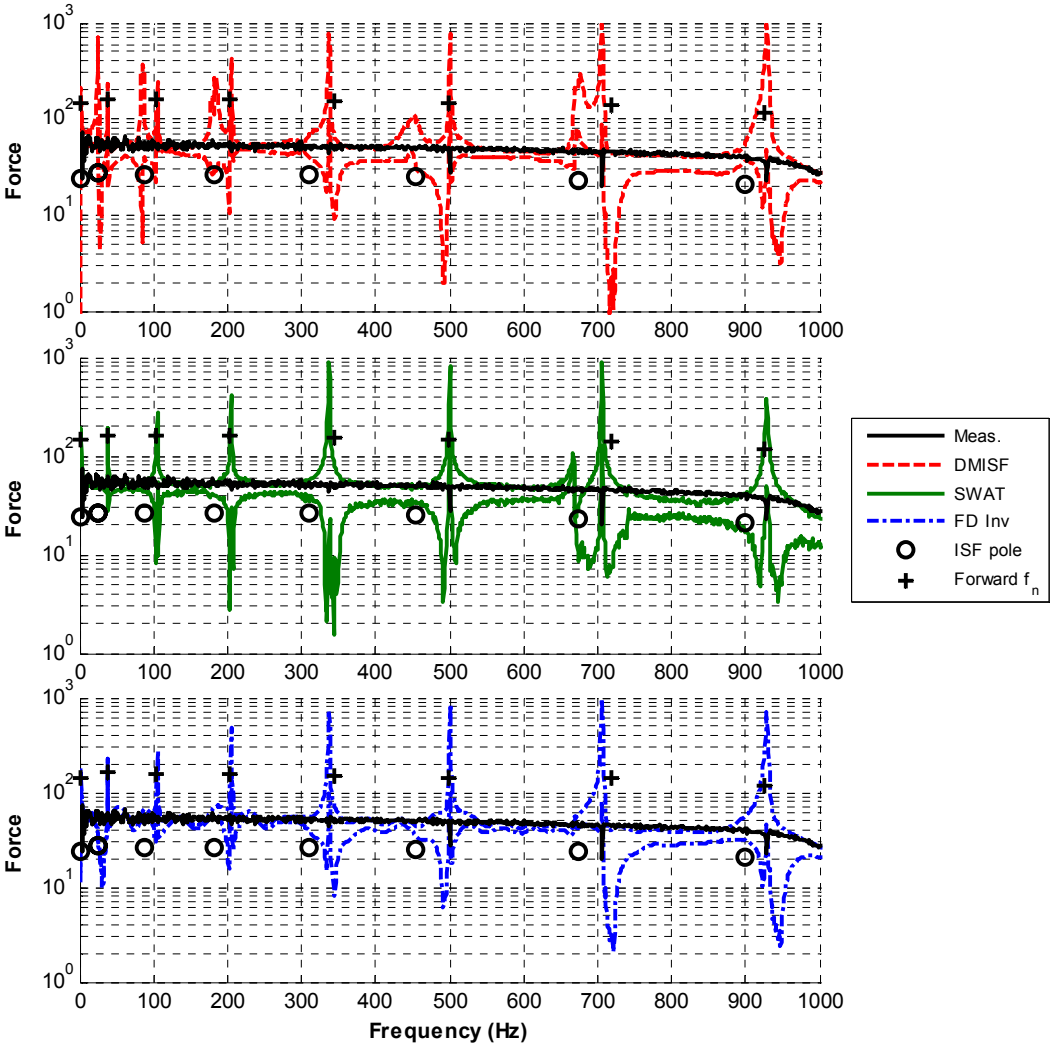

Figure 10: Range of forces found versus frequency for DMISF (top), SWAT (middle) and Frequency Domain Inverse method (bottom).

3.5.1. Discussion

It is interesting to note that all of the methods are sensitive at the natural frequencies of the forward system. While this is easily explained for the FD method based on the rank of the FRF matrix at resonance [5], it is perhaps surprising that the same is true for the ISF and SWAT methods, which are computed in a totally different way. Yet the results show that all three methods have about the same level of scatter at the forward system natural frequencies. This seems to indicate a conservation of difficulty for the inverse problem, regardless of the way in which it is computed. On the other hand, the time

domain force pulse was computed most accurately with the DMISF method, where the other two methods seemed to exhibit bias errors due to errors in the forward system parameters.

One drawback to the DMISF method, is that it also shows high sensitivity at its pole frequencies. This sensitivity was even more severe when the number of delays used (p in eq. (4)) was less than nine. In practice, the maximum number of delays used will be limited by available computing power. Fortunately, there are other avenues that can be explored [10] to better place the poles of the ISF to limit its sensitivity.

There are also implementation issues that one must consider. For example, only the SWAT and DMISF algorithms are capable of estimating the forces in the time domain. One should also note that the SWAT algorithm is much more computationally efficient than any of the other methods.

4. Conclusions

This work presented an enhancement to the Inverse Structural Filter (ISF) dubbed the Delayed, Multi-step ISF (DMISF). The performance of the DMISF was demonstrated using laboratory test data for a simple free beam. The forces identified by the DMISF were compared with those identified by the Sum of Weighted Accelerations Technique (SWAT) and by the classical Frequency Domain (FD) inverse method. The FD method was included as a reference because it is widely used and many researchers are familiar with it. In the applications of interest real time estimates of the forces are needed, so one would have to choose between the time domain algorithms (SWAT, ISF and DMISF). The ISF of Kammer and Steltzner was shown to accurately predict the force impulse applied to the structure, yet the forces that it predicted contained a spurious, large amplitude ringing after the force impulse had ceased. Both the DMISF and the FD method more accurately predicted the force impulse with significantly less residual ringing. For the DMISF, the residual ringing was found to be a function of the damping in the poles of the DMISF system. The damping in these poles increased as the number of delays used in the filter was increased; the poles were unstable for small p, becoming stable for $p > 8$, and increasingly heavily damped for even larger p. This ability to modify the stability of the filter is a key advantage of the

DMISF. No such recourse exists for the standard ISF when a forward system model is used as initial data.

One key advantage of the DMISF over the ISF stems from the way it is computed. The original ISF presented by Kammer and Steltzner was derived directly from the measured impulse response, whereas this new DMISF was derived from a state space model of the forward dynamic system. For the problem presented here, the forward dynamic system model was identified using the Algorithm of Mode Isolation, yet one is free to use any of a number of well developed system identification algorithms. The discussion of the identification process that was performed demonstrated the care that must be taken to obtain an adequate forward system model. This is far more likely to be achieved if one is free to use the tools or software packages that one is familiar with. The original ISF did not provide this latitude.

The sensitivity of the DMISF, SWAT and FD algorithms to errors in the forward system model was also investigated for the system of interest using a Monte Carlo Simulation (MCS). All of the methods exhibited relatively little scatter over the duration of the force impulse, with the DMISF being the most accurate on average and the FD and SWAT methods over and under predicting the magnitude of the impulse. A comparison of the force spectra revealed high scatter in the estimated forces at the natural frequencies of the forward system for all of the methods. This seems to be a general limitation of this type of analysis. Fortunately, the spectrum of a force that is of short duration will be smooth at frequencies that are much lower than the inverse of the force's duration. When this is the case the errors near the structure's natural frequencies are more of a nuisance than a real problem because they can be ignored or corrected by smoothing or windowing. On the other hand, a force spectrum that has significant narrowband components could be quite difficult to accurately identify using these methods.

It is often emphasized that the inverse problem is highly sensitive to errors in the parametric model for a structure, and thus implied that one should abandon any hopes of obtaining reasonable results. This work has demonstrated that it is more accurate to say that the inverse problem is sensitive to errors in quantities that are not important for some other applications. Many applications of experimental modal analysis, such as FEA model validation, may be able to tolerate relatively large errors in the natural

frequencies and mode shapes of the system under test, leading to much less stringent system identification requirements. On the other hand, the ISF and FD methods were found to be sensitive to the zeros of the forward system and there were nuisance issues associated with the effects of modes below the frequency band of interest, so attention had to be given to these issues. Control system design and admittance modeling are two more examples of applications that can also be sensitive to errors in the zeros of a system. These applications are certainly more difficult, yet one should not give up hope. More than adequate results can be obtained in many cases, especially if the limitations and sensitivities of the methods are understood and accounted for.

5. Appendix

5.1. ISF from Modal Parameters

One common approach for identifying a forward model for a linear time invariant system is to fit measured Frequency Response Functions (FRFs) $H(\omega)$ to a state-space modal model according to the following standard definition [38, 39]

$$[H(\omega)]_{N_o \times N_i} = \sum_{r=1}^{N/2} \left(\frac{[A]_r}{i\omega - \lambda_r} + \frac{[A^*]_r}{i\omega - \lambda^*_r} \right) \tag{12}$$

where $()^*$ denotes the complex conjugate, ω denotes the frequency, and λ_r is the modal eigenvalue of the rth mode of vibration. The eigenvalue is related to the modal natural frequency ω_r and modal damping ratio ζ_r by $\lambda_r = -\zeta_r \omega_r + \omega_r (1-\zeta_r^2)^{1/2}$. The residue matrices $[A]_r$ are defined in terms of the displacement portion of the state space mode vector $\{\psi\}_r$. The elements of the mode vector corresponding to the N_i drive locations $\{\psi_{drive}\}_r$ and the N_o response locations $\{\psi_{resp}\}_r$ are used to define the residue matrix as follows (using the normalization described by Ginsberg [40]).

$$[A]_r = \lambda_r \{\psi_{resp}\}_r \{\psi_{drive}\}_r^T \tag{13}$$

If the forces are applied at a subset of the response locations, then the mode vector can be expressed as

$$\begin{aligned} \{\psi\}_r &= \{\psi_{resp}\}_r \\ \{\psi_{drive}\}_r^T &= \{\psi\}_r^T [F_{in}] \end{aligned} \tag{14}$$

where $[F_{in}]$ is typically a N_o x N_i matrix of ones and zeros that selects the subset of the response locations at which forces are applied.

The experimentally derived modal model can be related to a state space model as in eq. (1) in a number of ways. For example, one can use the Laplace domain representation of eq. (12) to show that the following continuous-time state space system generates the Frequency response function in eq. (12).

$$\begin{aligned} \{\dot{x}\} &= [A_c]\{x\} + [B_c]\{u\} \\ \{y\} &= [C_c]\{x\} \\ [A_c] &= \begin{bmatrix} \Lambda & \\ & \Lambda^* \end{bmatrix} \quad [B_c] = \begin{bmatrix} \Psi\Lambda & \Psi^*\Lambda^* \end{bmatrix}^T [F_{in}] \\ [C_c] &= \begin{bmatrix} \Psi & \Psi^* \end{bmatrix} \end{aligned} \tag{15}$$

In the preceding equation, $[\Lambda]$ is a diagonal matrix containing the eigenvalues in ascending order and the columns of $[\Psi]$ contain the mode vectors $\{\psi\}_r$ in the same order as the eigenvalues. The subscript 'c' denotes that these are the state space matrices for the continuous time representation, in contrast to the discrete time matrices in eq. (1).

Before proceeding to the discrete time representation, we note that acceleration is most commonly measured, although eq. (15) relates displacement to the input force. One can modify the representation in eq. (15) to arrive at a state space representation for acceleration measurements by taking two derivatives of the output equation and substituting the derivative of the state equation. The following state space representation results.

$$
\begin{aligned}
&\{\ddot{x}\} = [A_c]\{\dot{x}\} + [B_c]\{\dot{u}\} \\
&\{\ddot{y}\} = [C_c]\{\ddot{x}\} = [C_c]\left([A_c]\{\dot{x}_c\} + [B_c]\{\dot{u}\}\right) \\
&\{\ddot{y}\} = [C_A]\{\dot{x}\} + [D_A]\{\dot{u}\} \\
&[C_A] = \begin{bmatrix} \Psi\Lambda & \Psi^*\Lambda^* \end{bmatrix} \quad [D_A] = [C_c][B_c] \\
&[D_A] = 2\,\mathrm{Re}\left(\Psi\Lambda\Psi^T\right)[F_{in}]
\end{aligned}
\tag{16}
$$

The new state vector is the derivative of the state vector in eq. (15). The input vector in eq. (16) is the derivative of the applied forces. Once inverted, the system in eq. (16) will estimate the derivative of the input forces from the acceleration measurements. These estimates must then be integrated numerically to obtain the input forces. It is generally accepted that numerical integration is less sensitive to errors than differentiation, although difficulties might occur as discussed in [41]. When performing this integration, the initial force must be known. (It is typically taken to be zero.)

A discrete time dual to the system representation in eq. (16) must be obtained in order to generate a discrete time inverse structural filter using eq. (2). The following discrete time representation will exactly reproduce the output of the continuous time system at the sample instants, if the input is constant between samples (zero-order-hold (ZOH) approximation) [26].

$$
\begin{aligned}
&\{x_{k+1}\} = [A]\{\dot{x}_k\} + [B]\{\dot{u}_k\} \\
&\{\ddot{y}_k\} = [C]\{\dot{x}_k\} + [D]\{\dot{u}_k\} \\
&[A] = \exp(A_c T_s) \quad [B] = [A_c]^{-1}\left[\exp(A_c T_s) - [I]\right][B_c] \\
&[C] = [C_A] \quad [D] = [D_A]
\end{aligned}
\tag{17}
$$

Note that because $[A_c]$ is generally diagonal (if the system is not defective), the matrix exponential of $[A_c]$ is a diagonal matrix with the discrete time eigenvalues $z_r = exp(\lambda_r T_s)$ along its diagonal.

Acknowledgments

This work was performed at Sandia National Laboratories and supported by the US Department of Energy under contract DE-AC04-94AL85000. The authors would like to thank Eric Stasiunas for providing the test data that was used in this work.

References

[1] K. K. Stevens, "Force Identification Problems - An Overview," in *Proceedings of the 1987 SEM Spring Conference on Experimental Mechanics*, Houston, TX, 1987, pp. 838-844.

[2] G. Genaro and D. A. Rade, "Input Force Identification in the Time Domain," in *16th International Modal Analysis Conference (IMAC XVI)*, Santa Barbara, California, 1998, pp. 124-129.

[3] R. J. Hundhausen, D. E. Adams, M. Derriso, P. Kukuchek, and R. Alloway, "Transient Loads Identification for a Standoff Metallic Thermal Protection System Panel," in *23rd International Modal Analysis Conference (IMAC XXIII)*, Orlando, Florida, 2005.

[4] J. A. Fabunmi, "Effects of Structural Modes on Vibratory Force Determination by the Pseudoinverse Technique," *AIAA Journal,* vol. 24, pp. 504-509, 1986.

[5] H. Lee and Y.-s. Park, "Error Analysis of Indirect Force Determination and a Regularisation Method to Reduce Force Determination Error," *Mechanical Systems and Signal Processing,* vol. 9, pp. 615-633, 1995.

[6] D. C. Kammer, "Input force reconstruction using a time domain technique," in *AIAA Dynamics Specialists Conference*, Salt Lake City, UT, 1996, pp. 21-30.

[7] B. Hillary and D. J. Ewins, "The Use of Strain Gauges in Force Determination and Frequency Response Function Measurements," in *2nd International Modal Analysis Conference (IMAC II)*, Orlando, Florida, 1984, pp. 627-634.

[8] E. Parloo, P. Verboven, P. Guillaume, and M. Van Overmeire, "Force Identification by means of in-operation modal models," *Journal of Sound and Vibration,* vol. 262, pp. 161-173, 2003.

[9] Q. Zhang, R. J. Allemang, and D. L. Brown, "Modal Filter: Concept and Applications," in *8th International Modal Analysis Conference (IMAC VIII)*, Kissimmee, Florida, 1990, pp. 487-496.

[10] M. S. Allen and T. G. Carne, "Comparison of Inverse Structural Filter (ISF) and Sum of Weighted Accelerations Technique (SWAT) Time Domain Force Identification Methods," in *47th AIAA-ASME-ASCE-AHS-ASC Structures, Structural Dynamics, and Materials Conference*, Newport, RI, 2006.

[11] V. I. Bateman and T. G. Carne, "Force Reconstruction for Impact Tests of an Energy-Absorbing Nose," *The International Journal of Analytical and Experimental Modal Analysis,* vol. 7, pp. 41-50, 1992.

[12] T. G. Carne, V. I. Bateman, and R. L. Mayes, "Force Reconstruction Using a Sum of Weighted Accelerations Technique," in *10th International Modal Analysis Conference (IMAC X)*, San Diego, CA, 1992, pp. 291-298.

[13] D. C. Kammer and A. D. Steltzner, "Structural identification of Mir using inverse system dynamics and Mir/shuttle docking data," *Journal of Vibration and Acoustics,* vol. 123, pp. 230-237, 2001.

[14] D. C. Kammer and A. D. Steltzner, "Structural identification using inverse system dynamics," *Journal of Guidance Control and Dynamics,* vol. 23, pp. 819-825, 2000.

[15] A. D. Steltzner and D. C. Kammer, "Input Force Estimation Using an Inverse Structural Filter," in *17th International Modal Analysis Conference (IMAC XXVII)*, Kissimmee, Florida, 1999, pp. 954-960.

[16] S. S. Law and T. H. T. Chan, "Moving Force Identification: A Time Domain Method," *Journal of Sound and Vibration,* vol. 201, pp. 1-22, 1997.

[17] J. P. Caffrey, S. F. Masri, F. Tasbihgoo, A. W. Smyth, and A. G. Chassiakos, "A Re-Configurable Test Apparatus for Complex Nonlinear Dynamic Systems," *Nonlinear Dynamics,* vol. 36, pp. 181-201, 2004.

[18] S. W. R. Duym, J. F. M. Schoukens, and P. A. N. Guillaume, "A local restoring force surface method," *The International Journal of Analytical and Experimental Modal Analysis,* vol. 11, pp. 116-132, Dec 1996.

[19] S. F. Masri, J. P. Caffrey, T. K. Caughey, A. W. Smyth, and A. G. Chassiakos, "Identification of the state equation in complex non-linear systems," *International Journal of Non-Linear Mechanics,* vol. 39, pp. 1111-1127, 2004/9 2004.

[20] S. F. Masri and T. K. Caughey, "A Nonparametric Identification Technique for Nonlinear Dynamic Problems," *Journal of Applied Mechanics,* vol. 46, pp. 433-447, 1979.

[21] P. E. Hollandsworth and H. R. Busby, "Impact Force Identification Using the Generalize Inverse Technique," *International Journal of Impact Engineering,* vol. 8, pp. 315-322, 1989.

[22] J. Schoukens, R. Pintelon, and H. Van hamme, "Identification of Linear Dynamic Systems Using Piecewise Constant Excitations: Use, Misuse and Alternatives," *Automatica,* vol. 30, pp. 1153-1169, 1994.

[23] D. J. Ewins, *Modal Testing: Theory, Practice and Application*. Baldock, England: Research Studies Press, 2000.

[24] S. Maia, J. M. M. Silva, J. He, N. A. Lieven, R. M. Lin, G. W. Skingle, W. M. To, and A. P. V. Urgueira, *Theoretical and Experimental Modal Analysis*. Taunto, Somerset, England: Research Studies Press Ltd., 1997.

[25] B. Peeters, "System Identification and Damage Detection in Civil Engineering," Leuven: Katholeike Universiteit Leuven, 2000, p. 256.

[26] K. Ogata, *Discrete-time control systems*, 2nd Edition ed. Upper Saddle River, New Jersey: Prentice Hall, 1994.

[27] D. L. Gregory, T. G. Priddy, and D. O. Smallwood, "Experimental Determination of the Dynamic Forces Acting on Non-Rigid Bodies," in *Aerospace Technology Conference and Exposition*, Long Beach, California, 1986, p. SAE Paper 861791.

[28] D. O. Smallwood and D. L. Gregory, "Experimental Determination of the Mass Matrix Using a Constrained Least Squares Solution," in *AIAA/ASME SDMC Conference*, Monterey CA, 1987.

[29] G. H. James, "Estimation of the Space Shuttle Rollout Forcing Function," in *23rd International Modal Analysis Conference (IMAC XXIII)*, Orlando, Florida, 2005.

[30] R. L. Mayes, "Measurement of Lateral Launch Loads on Re-Entry Vehicles Using SWAT," in *12th International Modal Analysis Conference (IMAC XII)*, Honolulu, Hawaii, 1994, pp. 1063-1068.

[31] M. S. Allen, "Global and Multi-Input-Multi-Output (MIMO) Extensions of the Algorithm of Mode Isolation (AMI)," in *George W. Woodruff School of Mechanical Engineering* Atlanta, Georgia: Georgia Institute of Technology, 2005, p. 129.

[32] M. S. Allen and J. H. Ginsberg, "Global, Hybrid, MIMO Implementation of the Algorithm of Mode Isolation," in *23rd International Modal Analysis Conference (IMAC XXIII)*, Orlando, Florida, 2005.

[33] M. S. Allen and J. H. Ginsberg, "Modal Identification of the Z24 Bridge Using MIMO-AMI," in *23rd International Modal Analysis Conference (IMAC XXIII)*, Orlando, Florida, 2005.

[34] M. S. Allen and J. H. Ginsberg, "A Global, Single-Input-Multi-Output (SIMO) Implementation of The Algorithm of Mode Isolation and Applications to Analytical and Experimental Data," *Mechanical Systems and Signal Processing,* vol. 20, pp. 1090–1111, 2006.

[35] W. Heylen, S. Lammens, and P. Sas, *Modal Analysis Theory and Testing*. Leuven, Belgium: Katholieke Universiteit Leuven, 2000.

[36] R. J. Allemang, *Vibrations Course Notes*. Cincinnati: http://www.sdrl.uc.edu/, 1999.

[37] B. Peeters and G. D. Roeck, "Stochastic System Identification for Operational Modal Analysis: A Review," *Journal of Dynamic Systems, Measurement, and Control,* vol. 123, December 2001.

[38] R. J. Allemang and D. L. Brown, "A Unified Matrix Polynomial Approach to Modal Identification," *Journal of Sound and Vibration,* vol. 211, pp. 301-322, 1998.

[39] R. Pintelon and J. Schoukens, *System Identification: a frequency domain approach*. Piscataway, NJ: IEEE Press, 2001.

[40] J. H. Ginsberg, *Mechanical and Structural Vibrations*, First ed. New York: John Wiley and Sons, 2001.

[41] T. S. Edwards, "Effects of aliasing on numerical integration," *Mechanical Systems and Signal Processing,* vol. in press, 2006.